



HAL
open science

Premixed flame dynamics in presence of mist

Colette Nicoli, Pierre Haldenwang, Bruno Denet

► **To cite this version:**

Colette Nicoli, Pierre Haldenwang, Bruno Denet. Premixed flame dynamics in presence of mist. *Combustion Science and Technology*, 2019, 191 (2), pp.197-207. 10.1080/00102202.2018.1453728 . hal-01820207

HAL Id: hal-01820207

<https://hal.science/hal-01820207>

Submitted on 21 Jun 2018

HAL is a multi-disciplinary open access archive for the deposit and dissemination of scientific research documents, whether they are published or not. The documents may come from teaching and research institutions in France or abroad, or from public or private research centers.

L'archive ouverte pluridisciplinaire **HAL**, est destinée au dépôt et à la diffusion de documents scientifiques de niveau recherche, publiés ou non, émanant des établissements d'enseignement et de recherche français ou étrangers, des laboratoires publics ou privés.

Premixed flame dynamics in presence of mist

Colette Nicoli, Pierre Haldenwang*,
Aix Marseille Université, CNRS, Centrale Marseille,
M2P2 UMR 7340, 13451, Marseille, France

and

Bruno Denet
Aix Marseille Université, CNRS, Centrale Marseille,
IRPHE UMR 7342, 13384, Marseille, France

June 21, 2018

Abstract

5 The injection of a water spray within an enclosure prone to explosion is reputed to reduce the risk. This strategy for safety improvement is at the root of numerous experiments that have concluded that premixed flame can be extinguished by a sufficient amount of a water aerosol characterized by suitable droplet sizes. On the other hand,
10 certain experiments seemingly indicate that flame speed promotion can be observed when particular water mists are injected within the premixture.

 To contribute to shed light upon these less than intuitive observations, we propose to study the propagation of a nearly stoichiometric premixed flame within a 2D-lattice of water droplets. Main parameters
15 of investigation are droplet size and droplet inter-distance (or equivalently, lattice spacing). When the droplet inter-distance is small, the results confirm that a sufficient amount of water quenches combustion. For larger droplet inter-distance, we observe a flame speed enhancement for suitable droplet size. Concomitantly, the flame front folds
20 subjected to Darrieus-Landau instability. The final discussion, which invokes a Sivashinsky-type model equation for DL instability, interprets such a speed promotion in presence of mist as a secondary non-linear enhancement of the flame surface.

*Corresponding author

25

keyword:

Water-sprayed flame; misted flame; flame mitigation; premixed flame speed-up; Darrieus-Landau instability

1 Introduction

30

Deflagration of fuel–air mixture is an omnipresent threat in the enclosures that contain industrial processes or energy production systems. To prevent or mitigate the risk of explosion, systems of water sprinkling are expected to be efficient devices for safety. As a matter of fact, numerous experiments have studied the propagation of a flame within a premixture composed of air, gaseous fuel and water mist. The situation corresponds to the so-called

35

”misted” flame.

40

It has clearly been established that the interaction between these components can lead to quench deflagration and/or detonation [Thomas et al., 1990, 1991], to mitigate gas explosion [van Wingerden et al., 1995], or to extinguish diffusion flame [Shimizu et al., 2001]. In other situations, pre-mixed flame interaction with water mist can delay the transition to detonation [Boeck et al., 2015]. The interaction can be restricted to only modify the structure of the deflagration [Thimothée et al., 2016] or the detonation [Jarsalé et al., 2016]. Microgravity facilities offer an ideal environment

45

for controlling the water spray characteristics and studying the effects of a quiescent water mist on the propagation of a premixed flame [Abbud-Madrid et al., 2001, Thimothée et al., 2016], the objective being the deduction of quantitative data about the effects of mean droplet inter-distance and droplet radius on extinction.

50

On the other side, and surprisingly, experimentalists often report on the opposite effect: injection of water mist can promote flame propagation [Gieras, 2008, Zhang et al., 2014]. In these articles, the aerodynamic effects produced by the injection of water droplets are invoked for creating large scale turbulence inside the premixture, and resulting in an acceleration of the flame propagation. By contrast with this interpretation, which involves

55

turbulence added by the mist injection, the purpose of the present contribution is to show that premixed acceleration is also possible with quiescent water mist, and to conclude that water droplets can intrinsically accelerate a flame already subjected to the Darrieus-Landau instability.

60

More generally, since fuel storage in liquid phase is known to achieve -for the time being- the best ratio of energy to weight, spray combustion is at the root of a wide field of research. This has long motivated numerous investi-

gations dealing with liquid-injected combustion and spray-flame dynamics. The present numerical investigation follows a series of studies dedicated to fuel/air spray-flames. To schematize the initial state of the premixture, we have proposed to consider the fuel/air spray as a 2D-lattice, at the nodes of which fuel droplets are located. A set of contributions [Nicoli et al., 2014, 2015, 2016, Thimothée et al., 2017] has investigated the various roles played by the main spray parameters: s , the lattice spacing, φ , the equivalence ratio of the fuel-air premixture that initially surrounds the droplets, and R_d , the typical droplet radius.

By contrast with those contributions, we presently consider a single-phase premixed flame (i.e. with no fuel in liquid phase) which interacts with "passive" droplets of water. Actually, the present contribution can be seen as directly inspired by our most recent paper [Nicoli et al., 2017] that shows that "passive fuel" droplets are able to first trigger the Darrieus-Landau instability, then induce secondary small-scale non-linear perturbations which provoke additional flame speed-up. Fuel droplets are considered as "passive" when their vaporization is too slow for participating to propagation. This can be met in rich sprays where the so-called "spray Péclet number" is large [Nicoli et al., 2017].

The present topic consists in substituting water droplets for "passive fuel droplets". We can here select a near stoichiometric flame $\varphi = 1.1$ and droplets that can vaporize in such way that they are able to interact with the flame propagation. In other words, the numerical approach considers the mist as a thermal sink, and -when vaporizing- the droplet surroundings become diluted and colder loci where combustion slows down, or even is quenched. Since the presently selected chemical scheme is elementary, we are aware that the chemical role played by water on flame slowdown will not be taken into account. It is however admitted that this effect is generally limited, since it is known that injecting a steam rather than a spray is less efficient in flame quenching (see the review in Ref. [Crayford, 2004]).

2 Model for premixed flame propagation through a water droplet lattice

The article is based on 2D numerical simulations, which start from the basic equations characterizing any reactive medium. The model of spray-flame propagation resorts to the general approach we have used in the contributions [Nicoli et al., 2014, 2015]. The initial state of the spray is schematized by a 2D face-centered lattice, at the nodes of which water droplets are posi-

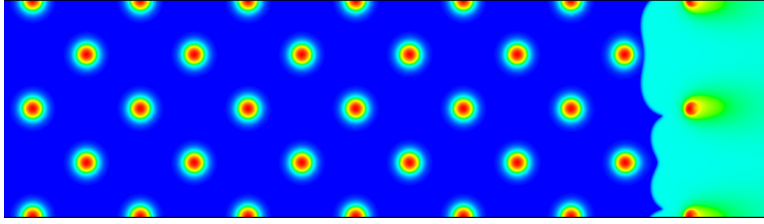


Figure 1: Water droplet 2D-lattice: H₂O mass fraction. On the left side of the figure, the initial field results from the positioning of the droplets at the nodes of a face-centred 2D-lattice of spacing s . On the right side, a nearly planar single-phase premixed flame propagates to the left ($\varphi = 1.1$, $R_d = 1.09$, $s = 12$). The computational domain represented is $L_y = 2 \times s$ high and $L_x = 7.1 \times s$ long.

100 tioned. The lattice spacing is denoted by s , in such a way that the droplet
inter-distance is $L_d = s/\sqrt{2}$. The spray-flame propagation is governed by
the usual set of conservation laws for mass, momenta, energy and species,
with the simplest chemical scheme [Nicoli et al., 2015] that allows us to han-
105 dle a flame propagating through a single-phase medium of heterogeneous
composition, where the equivalence ratio varies from φ far from the droplets
to an unknown value close to the droplets. As described in [Nicoli et al.,
2015], vaporization, Stefan flow and heat-mass transfers at the liquid-gas in-
terface are solved from the conservation laws and do not require particular
sub-models.

110 By contrast with most literature on spray-flames, the current droplets
are here fully resolved. This explains why 3-D DNS is hardly affordable for
a parametric exhaustive study. The droplets belong to the same continuum
as the gas; therefore, they can move, be carried by the flow, heat, follow the
properties of a real gas, and continuously switch from (liquid) dense fluid
115 to (vapour) light fluid; they also can distort themselves into non-circular
patterns, in absence of surface tension. The initial droplet radius varies
in a range from 0 to 2 in terms of flame thickness units δ_f^* : at standard
pressure, the droplets are hence submillimetric. The present simulation
takes advantage of the fact that surface tension is neglected: the liquid fuel
120 containment is simply achieved by the fact that heat and mass transfers are
frozen at the spray initial temperature (the spray being at rest far upstream
from the flame). The latter point is carried out by using the non-linear
dependence of the diffusion coefficients with respect to temperature. Lastly,
the latent heat of water is accounted for by a strongly non-linear dependence

125 of heat capacity with temperature. Note additionally that the experiments
in cloud Wilson chambers, carried out in microgravity [Thimothée et al.,
2016], lead to nearly monodisperse sprays, with a nearly regular density
for the droplets. This is why the current initial conditions are seemingly
relevant with regard to such experiments.

130 The chemical scheme and the implemented numerical methods have
largely been described in previous publications [Nicoli et al., 2015, 2017].
The set of equations, as well as the results we shall present, are handled
under non-dimensional form. The scales retained for non-dimensioning are
those of the adiabatic, stoichiometric, premixed flame of the considered fuel.
135 More precisely, the units for time, length, mass and temperature are derived
from the theoretical properties of this ideal flame, in terms of flame thick-
ness $\delta_f^* = D_{th,b}^*/U_L^*$, transit time $\tau_f^* = D_{th,b}^*/U_L^{*2}$, flame temperature T_b^* and
burnt gas density ρ_b^* . Hereinafter, the the subscript "u" is hence associated
with the fresh mixture, at the initial temperature T_u . The subscript "b"
140 is associated with the burnt mixture, at the flame temperature T_b . The
superscript "*" is associated with the values assessed for the adiabatic, sto-
ichiometric, single-phase flame.

The numerical experiments are conducted as follows. Water droplets are
initially positioned at the nodes of a face-centred lattice of spacing s (in δ_f^*
145 units), as illustrated by Fig.1. The lattice is embedded in a computational
box of length L_x and height L_y . For periodicity reason, we have chosen either
 $L_y = s$ or $L_y = 2s$. The surface tension of the droplets being neglected, a
droplet appears as a dense water puff belonging to the same continuum
as its surrounding premixture. Heat-mass transfers, vaporization and the
150 related gas expansion start when the medium is heated by the proximity
of the flame. Among the main quantities computed, the flame spreading is
considered. Since the front is strongly corrugated and changing in space and
time, we choose an averaged definition of the front position by performing
the partial integration of the temperature field in the transverse (periodic)
155 y -direction. We hence obtain the one-dimensional quantity $\langle T \rangle_y(x, t)$. We
then define $x_F(t)$, the "mean flame" position at time t , as the locus where
 $\langle T \rangle_y(x_F, t) = 0.5$. U , the flame spreading rate, is hence $\dot{x}_F(t)$, the derivative
of $x_F(t)$.

3 Results

160 From the classical theory of DL-instability, it is known that the Darrieus-
Landau instability (DLI) presents a threshold in wavelength. This indicates

that the development of DL-instability within the framework of periodic conditions transverse to the propagation requires a wide enough "channel", namely that L_y , the imposed periodicity, should be of a few tens times as large as the flame thickness. Thus, before working with droplets, single-phase numerical experiments with strong initial noise have established that the minimal channel width allowing the DL-instability development, and denoted here by L_{DL} , presently corresponds to about 14 times the flame thickness (i.e. $L_{DL} \approx 14$). In other words, $L_y > L_{DL}$ is needed for observing the DL-instability in single-phase premixture, and the threshold $L_y = L_{DL}$ is the so-called cut-off scale of DL instability.

Next, we shall only consider transversally large box (i.e. $L_y > L_{DL}$). More precisely, L_y will take the values $L_y = 24, 36$ and 48 . As we shall always set $L_y = 2s = 2\sqrt{2}L_d$, the boxes will correspond to three cases of droplet inter-distance, which are hereafter called small, moderate and large droplet inter-distance L_d , respectively. In the course of its propagation, the premixed flame regularly meets the water droplets of the lattice. As can be observed in Fig.1, droplets of large size do not vaporize entirely when crossing the flame. As a result, the initial amount of liquid water is not the sole relevant parameter of the study, since it often does not fully interact with flame propagation. It directly acts for quenching only when the water droplet entirely vaporizes in the vicinity of the front, i.e. for small droplet radii or, more precisely, when the spray Péclet number is small enough. Hence, the main parameters are the droplet inter-distance -or the lattice spacing- and the droplet radius (or equivalently the water loading). In what follows, we give different fixed values to s , the lattice spacing, and vary the droplet radius. In the range of the studied parameters, we have observed flame extinction, flame mitigation, and flame acceleration.

3.1 Small droplet inter-distance

The figure 2 presents $x_F(t)$, the position of the "mean flame" against time, for $L_d = 12/\sqrt{2}$. The mean slope of these curves will be called flame speed. As can be remarked in the figure, when the flame meets a droplet, this can modify the instantaneous "mean flame" velocity, all the more so that the actual flame remains flat (normally to its propagation towards the x -direction). This is clearly the case of the curve for $R_d = 1.09$, the propagation of which is affected by the droplets. For the intermediate water loading $R_d = 2.18$, flame quenching occurs very early (actually, shortly after the lattice entrance). As for the smaller water loading obtained for $R_d = 0.545$, the flame

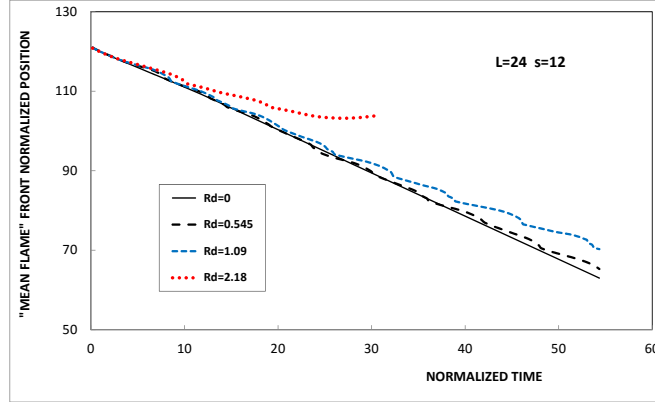


Figure 2: Small droplet inter-distance: position of the "mean flame" vs. time for several normalized radii of water droplets ($\varphi = 1.1$, $L_y = 24$, $s = 12$).

200 still propagates, being affected by the DL-instability. Its velocity appears slightly smaller than that without water loading. The figure 2 illustrates what is commonly accepted: water mist can quench or mitigate combustion spreading.

3.2 Moderate droplet inter-distance

205 Let us now consider the same variation of water droplet radii for the larger lattice spacing $s = 18$. The figure 3 again presents $x_F(t)$, the position of the "mean flame" against time. Only, the water loading of $R_d = 2.18$ is sufficient to quench the premixed flame (actually, the oscillations in the figure indicates that the "mean flame" position hesitates between two distinct positions just before extinction). On the other hand, a striking phenomenon of premixed flame acceleration occurs for the other water loadings. As a matter of fact, the mean slope for $R_d = 0.545$ and $R_d = 1.09$ appears faster that the single-phase flame non-loaded with water droplets (i.e. $R_d = 0$). In other words, only big droplets can affect a zone large enough for quenching the flame. Contrarily, when this zone is limited, it ends up with the slight
 215 enhancement of the premixed velocity. Here, the increase remains modest, being estimated to equal about 10%.

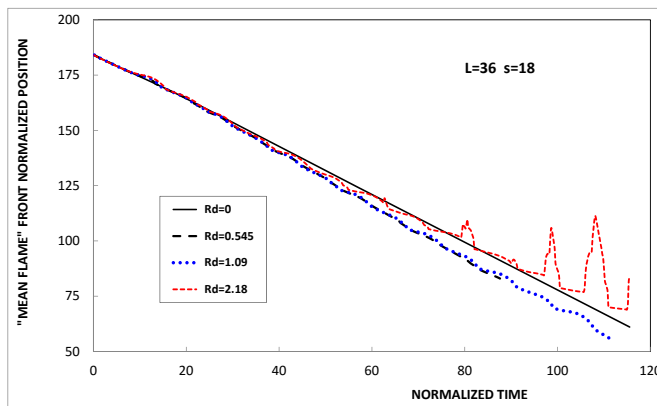


Figure 3: Moderate droplet inter-distance: position of the "mean flame" vs. time for several normalized radii of water droplets ($\varphi = 1.1$, $L_y = 36$, $s = 18$).

3.3 Large droplet inter-distance

Here, we consider the largest lattice spacing ($s = 24$). We have once more
 220 studied the "mean flame" position versus time. The result is presented in
 Fig. 4 where $x_F(t)$ is drawn against time. We did not find any water loading
 that is sufficient to quench the premixed flame. More precisely, all the mean
 slopes for $R_d = 0.545$, $R_d = 1.09$ and $R_d = 2.18$ indicate that premixed
 flame propagates faster in the presence of water droplets, provided that the
 225 droplet inter-distance is suitable. In other words, the domain of influence of
 each droplet -essentially due to Stefan flow- is too small -in comparison with
 the flame surface- to damp or muffle the flame. Contrarily, the presence of
 water droplets is responsible of flame speed-up, which is here of 15%. In the
 forthcoming section, we discuss the mechanisms involved either in quenching
 230 or in speed promotion. Moreover, it will be shown that a flame speed-up
 larger than 50% can be expected in very large boxes.

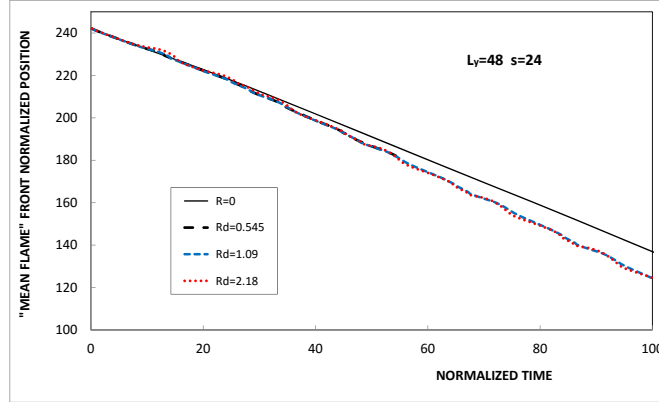


Figure 4: Large droplet inter-distance: position of the "mean flame" vs. time for several normalized radii of water droplets ($\varphi = 1.1$, $L_y = 48$, $s = 24$).

4 Discussion on mist effects

235 Evidently, the mechanism leading to extinguish a premixed flame resorts to the classical arguments for flame quenching, as the presence of efficient heat sinks. By contrast, the premixed flame acceleration by quiescent water mist requires a novel argumentation that necessitates new developments.

4.1 Mechanism for premixed flame extinguishing

240 In the course of its propagation through the lattice of water droplets, the flame front pattern results from the reconnection (or "wound healing") of two types of local behaviours: a) zones in the vicinity of the droplets, where a thermal sink is active and where the flame does not propagate, b) zones where the premixture seemingly can burn more or less adiabatically. If zones b) does exist, they burn even though they are submitted to lateral heat loss due to zones a). This picture relates to a classical problem: a premixed flame propagating in a channel which enforces heat losses at its walls. An approximate approach conducted with a simple diffusive-thermal model [Alliche et al., 2010] showed that -in a narrow channel of a given width- the premixed flame bends, all the more so that the lateral heat losses are large. There is nevertheless a critical value of the flame curvature radius,

245

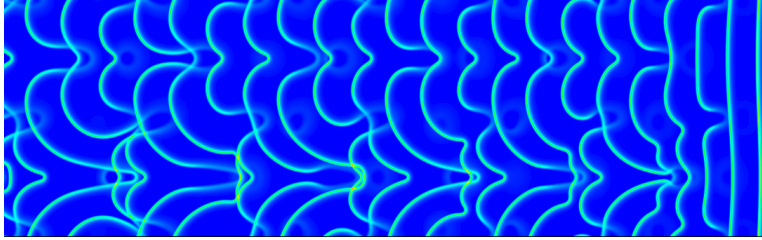


Figure 5: Superimposed successive snapshots of the reaction rate for a premixed flame, where DL-instability has been triggered by droplets ($\varphi = 1.1$, $R_d = 1.09$, $s = 24$ and $L_y = 48$).

below which quenching occurs.

In the previous section, flame extinction has been observed for $L_d = 12/\sqrt{2} \approx 8.5$. The model mentioned above [Alliche et al., 2010] predicted that propagation is allowed in a channel larger than seven times the flame
 255 thickness, whatever the strength of the thermal losses at the wall. Therefore, increasing moderately the droplet inter-distance will allow the propagation even for quite large water droplets. This is what happens when L_d is enlarged from $L_d = 12/\sqrt{2}$ to $L_d = 18/\sqrt{2}$ [resp. $L_d = 24/\sqrt{2}$] in paragraph 3.2 [resp. 3.3]. The latter situation is also considered in the next paragraph.

260 4.2 Flame "wound healing" and flame acceleration

Figure 5 illustrates the propagation (from the right to the left) of a premixed flame within the water droplet lattice: set initially flat, the flame front rapidly exhibits the classical cusped form of the flames subjected to Darrieus-Landau instability. Concomitantly, secondary wrinkles occur when
 265 the flame front meets a water droplet. Considering Fig.5, the mechanism now investigated starts from the following considerations: the droplet inter-distance is large, in such a way that the premixed flame possesses large zones of free propagation (i.e. more or less adiabatic). As observed for the rich spray-flames of the reference [Nicoli et al., 2017] in large boxes, "pas-
 270 sive" droplets trigger the Darrieus-Landau instability in the same manner as in Fig.5. This result was found in agreement with the classical results on DL instability, since the DL instability is known to require perturbations or noise to develop in a satisfactory manner [Denet and Haldenwang., 1995].

The presence of droplets can additionally provoke a more striking behaviour: the role of the droplets on the flame speed in the context of the
 275 fully-developed Darrieus-Landau instability. The DL instability in the non-

linearly saturated regime appears as a folded front with one cusp [sometimes with two cusps]. One cusp corresponds to the DL non-linear pattern with the fastest propagation. As described by Fig.5, such a front perturbed by
 280 "holes of no combustion" exhibits additional wrinkles of shorter wavelengths, which result from the wound healing of the DL-affected pattern drilled by the extinction holes that accompany the vaporizing droplets. Interpreted accordingly with a linear point of view in DL-theory, those short wavelengths would lead the spray-flame to a slower propagation. By contrast, a spreading
 285 enhancement is observed. This speed promotion has to be interpreted in a non-linear manner, in the sense that secondary wrinkles are additionally imposed to the fastest DL-pattern, and still increase the effective flame surface.

The last point is illustrated by Fig. 6, where three different quantities are
 290 gathered and compared. More precisely, \dot{x}_F , the flame mean front velocity as previously defined, is plotted against time in Fig.6.b, while the instantaneous overall heat release is drawn in Fig.6.a and whereas instantaneous flame surface area is depicted in Fig.6.c. In each sub-figure, we have plotted a moving average of the corresponding quantity performed on the floating
 295 time interval $[-10, 10]$, which more or less relates to the fluctuation period.

The quantity \dot{x}_F , as plotted in Fig.6.b, calls for the following comments. It presents large fluctuations which do not sound quite physical, especially the velocity fluctuations that become smaller than 1. This is certainly due to the artificial definition of x_F . Only the main values obtained by mov-
 300 ing average has a clear meaning; it exactly corresponds to the mean slope measured in Fig.4, i.e. what we have called "misted flame speed". To interpret the large fluctuations, we need the other two sub-pictures (6.a and 6.c), where the fluctuations appear rather in phase with those of \dot{x}_F (Fig.6.b). In Fig.6.c, the minimum value of the flame area is constant and more or less
 305 corresponds to that of the DL-pattern. This indicates that every increase in flame area is due the encounter of a droplet, the influence of which depends on the impact position along the DL-pattern. In others words, the local extinction due to a passive droplet increases the front area. After a
 "wound healing" process which depends on the droplet location along the
 310 DL-pattern, the front retrieves its more classical DL-pattern, and its corresponding velocity. As for the overall heat release plotted in Fig.6.a, its fluctuations confirm those of the surface, and show particularly complex peaks, the interpretation of which being not easy for the time being.

Note that the moving average of front velocity and heat release gives a
 315 rather constant value, while it is not exactly the case for the flame surface, for which a slight increase is observed. We interpret the drift as owing to

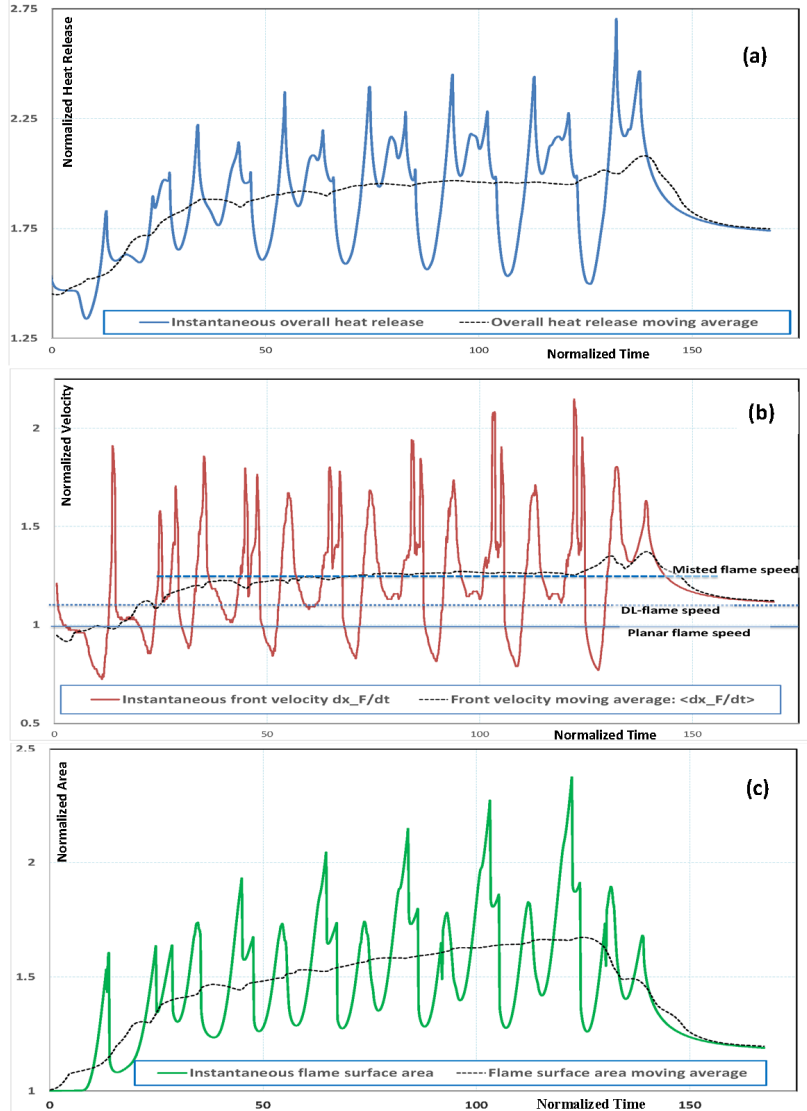


Figure 6: Comparison of three different instantaneous characterizations of flame spreading: (a) overall heat release, (b) \dot{x}_F , the flame mean front velocity, and (c) the overall flame surface area. Each quantity is additionally drawn (dotted line) smoothed by a moving average on a time interval of 20 normalized time units ($\varphi = 1.1$, $R_d = 1.09$, $s = 24$ and $L_y = 48$).

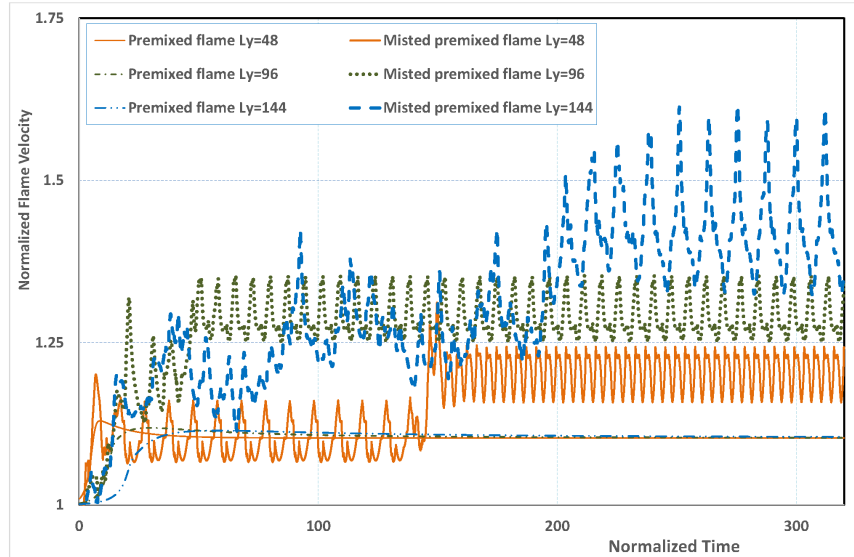


Figure 7: Premixed flame velocity vs. time as results of a Sivashinsky-like model equation in large boxes $L_y = 48, 96$ and 144 : the DL-velocities are compared with and without droplets (the droplets are modelled by holes of no combustion).

the droplet diffusion -as time goes- due to the absence of confinement by surface tension in our droplet model. The same argument might prevail for interpreting the shift in peak intensity in Fig.6.c. Nevertheless, the converging informations brought by Fig.6 confirm that the mist effects on the DL-affected premixed flame increase the flame front area, the combustion rate, and the flame velocity. As the flame velocity enhancement is clearly established, its strength remains rather modest: about 15%. We observed that the strength of the speed promotion increases with L_y . When L_y become very large, the numerical cost dramatically increases (all droplets are resolved!), and we decide to explore the tendency with a Sivashinsky-like model equation. This is the purpose of the forthcoming paragraph.

4.3 Further considerations for very large L_y

To make the study in large box affordable, we select the Sivashinsky-like model equation proposed by [Joulin and Cambray, 1992], which allows to handle DL-affected premixed flames with large amplitude wrinkles. The idea consists [Nicoli et al., 2017] in considering a propagation domain where

some local zones of no propagation are incorporated. After several attempts for choosing the size of the droplet influence zone, it turns out that varying
335 the size of the hole does not greatly change the results, provided that the size remains reasonably small in comparison with the lattice-spacing. The (costless) numerical experiments achieved with the model equation offer an evident theoretical sustainment to the numerical simulations: water droplets induce secondary wrinkles in the Darrieus-Landau pattern, which increase
340 the flame surface and promote the spreading velocity. The model equation parameters are then adjusted to retrieve the flame speed promotion observed in the simulations.

The (lateral) size of the box is now increased from $L_y = 48$ to $L_y = 144$, while the time of integration is prolonged. The results are reported in Fig.7.
345 The results of propagation without droplet exhibit the same asymptotic value whatever the box size. The value correspond to the DL-affect flame speed, i.e. $U_{DL} = 1.1$ (in adiabatic, stoichiometric, premixed flame speed units). When the flame is misted, the mean front speed oscillates with various frequencies. For instance for $L_y = 48$, as the flame meets droplets, its
350 velocity starts oscillating with a low frequency and exhibits no speed promotion, while asymptotically the frequency doubles and the speed increases to 1.2 as mean value. Such a non-linear behaviour appears complex and its study stands beyond the scope of the article. If the box size is doubled ($L_y = 96$), or tripled ($L_y = 144$), the mean value of the velocity oscillations
355 increases to 1.3 and 1.4 respectively. The latter value corresponds to a 30% enhancement. This gives cause for hope that much higher promotion can occur in combustion chamber of realistic size.

To sum-up, the present article shows a premixed flame dynamics in presence of mist, which is particularly rich: from extinction to acceleration. The
360 decisive parameter is the droplet inter-distance. When this quantity is small, a critical value of the water amount can quench the premixed flame. When the inter-distance is large, the droplets impose additional flame wrinkles to the Darrieus-Landau pattern. It results in flame speed-up.

365

Acknowledgements

The present work has received the support of the Research Program "Micropesanteur Fondamentale et Appliquée", GDR CNRS n2799, under contract CNES/170048.

370 **References**

- A Abbud-Madrid, EP Riedel, and JT McKinnon. The influence of water mists on premixed flame propagation in microgravity. In *Microgravity Research and Applications in Physical Sciences and Biotechnology*, volume 454, pages 313–320, 2001.
- 375 Mounir Alliche, Pierre Haldenwang, and Salah Chikh. Extinction conditions of a premixed flame in a channel. *Combustion and Flame*, 157(6):1060–1070, 2010.
- LR Boeck, A Kink, D Oezdin, J Hasslberger, and T Sattelmayer. Influence of water mist on flame acceleration, DDT and detonation in H₂-air mixtures.
380 *International Journal of Hydrogen Energy*, 40(21):6995–7004, 2015.
- Andrew Philip Crayford. *Suppression of methane-air explosions with water in the form of 'fine' mists*. PhD thesis, Cardiff University, 2004.
- B. Denet and P. Haldenwang. A numerical study of premixed flames Darrieus-Landau instability. *Combust. Sci. and Tech.*, 104:143–167, 1995.
- 385 Marian Gieras. Flame acceleration due to water droplets action. *Journal of Loss Prevention in the Process Industries*, 21(4):472–477, 2008.
- G Jarsalé, F Viot, and A Chinnayya. Ethylene–air detonation in water spray. *Shock Waves*, 26(5):561–572, 2016.
- G. Joulin and P. Cambray. On a tentative approximate evolution equation
390 for markedly wrinkled flames. *Combust. Sci. and Tech.*, 81:243–256, 1992.
- C. Nicoli, B. Denet, and P. Haldenwang. Lean flame dynamics through a 2D lattice of alkane droplets in air. *Combust. Sci. and Tech.*, 186(2):103–119, 2014.
- C. Nicoli, B. Denet, and P. Haldenwang. Rich spray-flame propagating
395 through a 2D-lattice of alkane droplets in air. *Combustion and Flame*, 162(12):4598–4611, 2015.
- C. Nicoli, B. Denet, and P. Haldenwang. Spray-flame dynamics in a rich droplet array. *Flow Turbulence and Combustion*, 96(2):377–389, 2016.
- Colette Nicoli, Pierre Haldenwang, and Bruno Denet. Darrieus-landau instability of premixed flames enhanced by fuel droplets. *Combustion Theory and Modelling*, 21(4):630–645, 2017.
400

- Hiroshi Shimizu, Manai Tsuzuki, Yasuo Yamazaki, and A Koichi Hayashi.
Experiments and numerical simulation on methane flame quenching by
water mist. *Journal of Loss Prevention in the Process Industries*, 14(6):
405 603–608, 2001.
- Romain Thimothée, Christian Chauveau, Fabien Halter, and Iskender
Gökalp. Experimental investigation of the mechanisms of cellular instabil-
ities developing on spherical two-phase flames. *Combustion Science and
Technology*, 188(11-12):2026–2043, 2016.
- 410 Romain Thimothée, Christian Chauveau, Fabien Halter, Colette Nicoli,
Pierre Haldenwang, and Bruno Denet. Microgravity experiments and nu-
merical studies on ethanol/air spray flames. *Comptes Rendus Mécanique*,
345(1):99–116, 2017.
- G. O. Thomas, M. J. Edwards, and D. H. Edwards. Studies of detonation
415 quenching by water sprays. *Combustion Science and Technology*, 71(4-6):
233–245, 1990.
- G. O. Thomas, A. Jones, and M. J. Edwards. Influence of water sprays
on explosion development in fuel-air mixtures. *Combustion Science and
Technology*, 80(1-3):47–61, 1991.
- 420 Kees van Wingerden, Brian Wilkins, Jrn Bakken, and Geir Pedersen. The
influence of water sprays on gas explosions. part 2: Mitigation. *Journal
of Loss Prevention in the Process Industries*, 8(2):61–70, 1995.
- Pengpeng Zhang, Yihui Zhou, Xingyan Cao, Xuliang Gao, and Mingshu Bi.
425 Enhancement effects of methane/air explosion caused by water spraying
in a sealed vessel. *Journal of Loss Prevention in the Process Industries*,
29:313–318, 2014.